

# Model-based Investigation of the Effect of the Cell Cycle on the Circadian Clock through Transcription Inhibition during Mitosis

Pauline Traynard, François Fages, Sylvain Soliman

Inria Paris-Rocquencourt, Team Lifeware, France

**Abstract.** Experimental observations have put in evidence autonomous self-sustained circadian oscillators in most mammalian cells, and proved the existence of molecular links between the circadian clock and the cell cycle. Several models have been elaborated to assess conditions of control of the cell cycle by the circadian clock, in particular through the regulation by clock genes of Wee1, an inhibitor of the mitosis promoting factor, responsible for a circadian gating of mitosis and cell division period doubling phenomena. However, recent studies in individual NIH3T3 fibroblasts have shown an unexpected acceleration of the circadian clock together with the cell cycle when the milieu is enriched in FBS, the absence of such acceleration in confluent cells, and the absence of any period doubling phenomena. In this paper, we try to explain these observations by a possible entrainment of the circadian clock by the cell cycle through the inhibition of transcription during mitosis. We develop a differential model of that reverse coupling of the cell cycle and the circadian clock and investigate the conditions in which both cycles are mutually entrained. We use the mammalian circadian clock model of Relogio et al. and a simple model of the cell cycle by Qu et al. which focuses on the mitosis phase. We show that our coupled model is able to reproduce the main observations reported by Feillet et al. in individual fibroblast experiments and use it for making some predictions.

## 1 Introduction

Most organisms, from bacteria to plants and animals, have a circadian clock present in each cell, generally in the form of a self-sustained genetic oscillator entrained by the day/night cycle through various mechanisms. This circadian clock has many effects on the cell including its metabolism [13]. Experimental results have also shown a regulation of the cell division cycle by the circadian clock [16,2,23], with possible applications to cancer chronotherapies [1,7]. Molecular links between these two cycles have been exhibited to explain this regulation. In particular the regulation of Wee1, an inhibitor of the mitosis promoting factor, by the clock genes, induces a circadian gating of mitosis to particular clock phases and can result in a synchronization of cell division with a 24h period or 48h period with period doubling phenomena [8]. Other similar molecular links going in the same direction, through p21 [14] and cMyc [17], have been shown

in the literature. A few models have also been developed to further investigate those hypotheses, by coupling a model of the cell cycle with a model of the circadian clock through those direct molecular links, and analyze the conditions of entrainment in period [12,6].

Several studies using large-scale time-lapse microscopy to monitor circadian gene expression and cell division events in real time and in individual cells during several days have unveiled unexpected behaviours, hinting that the relationship might be more complex. Nagoshi et al. [8] have first shown that circadian gene expression in fibroblasts continues during mitosis, but with a consistent pattern in circadian period variation relatively to the circadian phase at division, leading them to hypothesize that mitosis elicits phase shifts in circadian cycles. However, a more recent study of Bieler et al. [3] relating the same experiments on dividing fibroblasts found the two oscillators synchronized in 1:1 mode-locking leading the authors to hypothesize a predominant reverse coupling in NIH3T3 cells. This is in agreement with another study of Feillet et al. [11] which found several different synchronization states in NIH3T3 fibroblasts in different conditions of culture. It was observed there that enriching the milieu with Foetal Bovine Serum (FBS) not only accelerates the cell division cycle but also the circadian clock. For cells cultured in 10 % FBS, both distributions of the cell cycle length and the circadian clock are centered around 22h. For cells cultured in 15 % FBS, both the cell cycle and the circadian clock accelerate, with period distributions centered around 19h. However, when cells reach confluence and stop dividing, the circadian clock slows down and the period distribution is then centered around 24h. None of the currently available models coupling the cell cycle and the circadian clock can explain these observations since they are based on an unidirectional influence of the circadian clock on the cell cycle [12,6].

In this paper, we hypothesize that the inhibition of transcription during mitosis in eukaryotes [24] constitutes a reverse interaction from the cell cycle to the circadian clock, which can enable an entrainment of the circadian clock by the cell cycle and can explain the acceleration of the circadian clock in non-confluent cells when the concentration of FBS increases. We develop a differential model of this reverse coupling from the cell cycle to the circadian clock and investigate the conditions in which both cycles are mutually entrained. We use the mammalian circadian clock model of Relogio et al. [19] and a simple model of the cell cycle by Qu et al. [18] which focuses on the mitosis phase. We show that our coupled model is able to reproduce the observations on periods reported by Feillet et al. [11] in individual fibroblast without treatment by Dexamethasone. Furthermore we argue that the complex behaviors observed with high variability after treatment by Dexamethasone, modeled by the induction of a high level of *Per* and the inhibition of the other clock core genes, can be explained by the perturbation of the clock after this treatment. In our model, the stabilization time after that pulse appears to be greater than the time horizon used in those experiments. Our results are thus compatible with the observations on the periods and phase locking modes of [11], however, the observations on the precise phase shift between the mitosis time and the circadian clock *REV-ERB- $\alpha$*  pro-

tein peaks reported in [11] are not reproduced by our model, nor are they by the other coupled models of [12,6]. This intriguing remaining difficulty is discussed at the end of the paper.

The methodology used to perform these investigations is based on a formal specification of the observed behavior with temporal logic patterns [10,22] which are used in the BIOCHAM modeling environment [5] for parameter search [21] and robustness and sensitivity analysis [20]<sup>1</sup>.

## 2 Experimental Observations and their Specification in Temporal Logic

### 2.1 Experimental Data

In this section we explain the experiments and analysis performed in [11] and the conclusions drawn by the authors. The reported experiments have been done using cell tracking and time-lapse image analysis of various fluorescent markers of the cell cycle and the circadian clock observed during 72 hours in proliferating NIH3T3 mouse fibroblasts.

These cells were modified to include three fluorescent markers of the circadian clock and the cell cycle: the REV-ERB- $\alpha$ ::Venus clock gene reporter for measuring the expression of the circadian protein REV-ERB- $\alpha$ , and the Fluorescence Ubiquitination Cell Cycle Indicators (FUCCI), Cdt1 and Geminin, two cell cycle proteins which accumulate during the G1 and S/G2/M phases respectively, for measuring the cell cycle phases.

The cells were left to proliferate in regular medium supplemented with different concentrations of FBS (10%, 15% and 20%). Long-term recording was performed in constant conditions with one image taken every 15 minutes during 72 hours. Cell division times were also measured during the tracking of cell lineages. Cell cycle length was measured as the time interval between two consecutive cell divisions and a piece-wise linear model fitted to both markers of the cell cycle extracted the time of the G1-S transitions.

The expression traces of REV-ERB- $\alpha$  were detrended and smoothed, and spectrum resampling was used to estimate the clock period. Cells with less than two REV-ERB- $\alpha$  peaks within their lifetime, a period length outside the interval between 5 hours and 50 hours or a relative absolute error (RAE) bigger than 0.25 (showing a confidence interval wider than twice the estimated period) were classified as non-rhythmic and discarded, assuming that they do not have a functioning clock.

Furthermore, a series of experiments were done with a pulse of Dexamethasone (Dex) before recording. This glucocorticoid agonist is known to exert a resetting/synchronizing effect on the circadian molecular clocks in cultured cells through the induction of *Per1*. In that case the cells were incubated for 2 hours

---

<sup>1</sup> The models and the specification used in this paper are available on <http://lifeware.inria.fr/wiki/software/cmsb15>.

in the same medium supplemented with Dex, just before returning to a Dex-free medium for the recording.

The quantitative data on the periods of the cell cycle and the circadian clock are summarised in the table 1 [11]. Cells non-treated with dexamethasone show a similar period for the cell cycle and the circadian clock both in 10% and 15% FBS conditions. Interestingly, increasing FBS significantly decreases both mean periods of the clock and the cell cycle, from 21.9h to 19.4h and from 21.3h to 18.6h respectively, showing that both oscillators remain unexpectedly in 1:1 mode locking. While the speedup of the cell cycle can be directly attributed to the growth factors in increasing concentration of FBS, it can not account for the speedup of the clock the same way, since confluent cells keep a 24-hours period for the circadian clock independently of the FBS concentration.

Medium	No dexamethasone		Dexamethasone	
	Clock period	Division period	Clock period	Division period
<b>FBS 10</b>	21.9h $\pm$ 1.1h	21.3h $\pm$ 1.3h	24.2h $\pm$ 0.5h	20.1h $\pm$ 0.94h
<b>FBS 15</b>	19.4h $\pm$ 0.5h	18.6h $\pm$ 0.6h	NA	NA
<b>FBS 20</b>	NA	NA	21.25h	19.5h
<b>FBS 20</b>	NA	NA	29h	16h

**Table 1.** Estimated periods of the circadian molecular clock and the cell division cycle measured in [11] in fibroblast cells for various concentrations of FBS, with and without dexamethasone. The experiment done with 20% FBS have been clustered by the authors of [11] in two groups with different periods.

The results are more complex in the case of the cells treated with dexamethasone. Cells in 10% FBS show an increased clock period and a low cell cycle period, with an overall ratio of 5:4. In 20% FBS the cell lineages are dominated by two groups. The first group shows close periods, i.e. a 1:1 mode-locking similarly to the experiments without dexamethasone. The second group shows a high clock period and a fast cell cycle, with an overall ratio close to 3:2 between the clock and cell cycle, explaining the three-peaks distribution of the circadian phase, as already observed by Nagoshi et al.[8] ten years before. It has to be noted that the 20% FBS dexamethasone-synchronized experiment was repeated with similar results available in the Supplementary Information of [11], although the distribution of the period ratios for the second group is wider in the interval [1.2 – 2].

In [11], the authors suggest that these observations might be interpreted by the existence of distinct oscillatory stable states coexisting in the cell populations, in particular with 5:4 and 1:1 phase-locking modes for the condition 10% FBS, and 3:2 and 1:1 phase-locking modes for the condition 20% FBS, and that the dexamethasone could knock the state out of the 1:1 mode toward other attractors. A mechanistic explanation remains to be found to support this inter-

pretation. In this paper, we investigate a simpler hypothesis of entrainment of the circadian clock by cell divisions through the inhibition of transcription during mitosis and show with a model that this hypothesis can explain the observations on the periods.

## 2.2 Temporal Logic Specification

For the analysis of the dynamical behavior of the system, we rely on the formalisation of the oscillatory properties in quantitative temporal logic with simple formula patterns [10,22], which allow us to combine qualitative properties of oscillations and quantitative properties on the shapes of the traces such as distances between peaks or peak amplitudes. This is useful to capture the periods on both experimental and simulated traces, even when the traces are noisy. We use flexible constraints on the amplitudes and regularity of the peaks to filter out traces, keeping only sustained oscillations even with small irregularities, as it is the case for example on the Figure 7.

For instance, the following formula is used to compute the period of REV-ERB- $\alpha$  in a trace:

```
distanceSuccPeaks([RevErb::nucl],[period],[80]) &
Exists([maxdiff1,maxdiff2,maxpeak],
maxDiffDistancePeaks([RevErb::nucl],[maxdiff1],[80])
& maxDiffAmplPeaks([RevErb::nucl],[maxdiff2],[80])
& maxAmplPeaks([RevErb::nucl],[maxpeak],[80])
& 4*maxdiff1<period+errordiff1
& 10*maxdiff2<maxpeak+errordiff2
& maxpeak>0.1+errorampl)
```

The period constraint on the oscillations of REV-ERB- $\alpha$  is expressed by the formula pattern *distanceSuccPeaks*, whose validity domain provides all the values of the distances between peaks of concentrations of REV-ERB- $\alpha$  [10], after a transient time of 80h to avoid irregularities caused by the initial state.

Moreover, the formula patterns *maxDiffDistancePeaks*, *maxDiffAmplPeaks*, and *maxAmplPeaks* capture several variables characterizing irregularity features of the trace: *errordiff1* for the irregularities in distances between peaks, *errordiff2* for the irregularities in the amplitudes of the peaks, and *errorampl* for a small concentration amplitude. Setting then thresholds on these variables ensures that unwanted traces are filtered out.

These logical formulae can then be used in a modeling environment such as BIOCHAM [5] in a variety of ways for data analysis [9], model parameter search in high dimension and robustness and sensitivity measures [21,20,4].

## 3 Mathematical Models and their Coupling

### 3.1 Model of the Cell Cycle

The cell cycle of somatic cells is composed of four phases: DNA replication (S phase) and chromosome segregation or mitosis (M phase), separated by two gap

phases (G1 and G2). At the center of the cell cycle regulation, there is a group of proteins, the cyclin-dependent kinases, which are complexes composed of a kinase and a cyclin partner determining the specificity of the complex. Each phase of the cell cycle is controlled by a specific cyclin-dependent kinase.

For our purpose, it is sufficient to use a model focusing on the G2-M transition which leads to mitosis. We use a model proposed by Qu et al. [18] in which the cell cycle is divided in two different phases, the G1-S-G2 and M phases. The M phase is triggered by the complex CDC2/CYCLIN B. This complex appears in two forms, an active form called MPF (M-phase Promoting Factor) and a phosphorylated, inactive form called preMPF. MPF is phosphorylated and inactivated by the kinase WEE1, and dephosphorylated and activated by the phosphatase CDC25. Both the kinase and phosphatase activities are themselves regulated by MPF, respectively inactivated and activated by the complex.

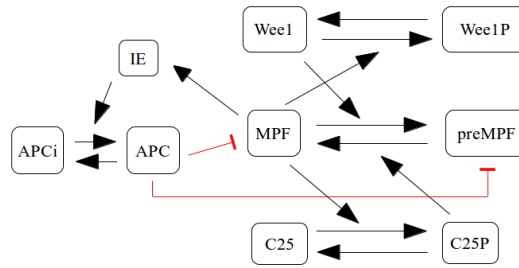


**Fig. 1.** Schema of the cell cycle model of Qu et al. [18].

The mechanism by which changing the concentration of FBS modulates the cell cycle length is unclear, and probably involves an increase in growth factors. In this model, we assessed the effect of each reaction rate constant on the period of the concentrations and found that two parameters were particularly significant to change the period: *kdie*, the degradation rate of the intermediary enzyme involved in the negative feedback loop between MPF and the proteasome APC, and *kampf*, the activation of MPF by CDC25P. Both are able to change widely the range of the cell cycle period without changing significantly the strength of the coupling, and should thus provide the same effect, so we choose one of them, *kampf*, to modulate the cell cycle period. We shall use the following values for *kampf*: 3.75 for a cell division period of 21.3 hours (corresponding to 10% FBS), 12.1 for a period of 18.6 hours (15% FBS).

More detailed models distinguishing the four phases of the cell cycle of course exist, such as [12] for instance, making possible to represent various regulations from the circadian clock genes, for instance through WEE1 during M-phase and through p21 and Cmyc during the S-phase. However, since the consequences of those regulations have not been observed in the experimental data described in

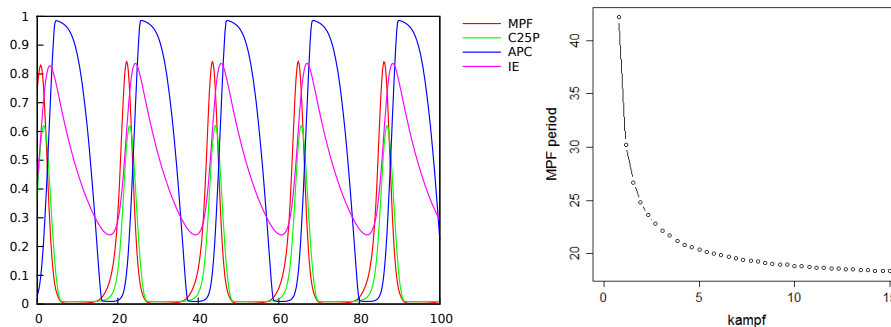


**Fig. 2.** **Left:** Simulation of the cell division cycle model of Qu et al. **Right:** Period of the cell division cycle (measured as the distance between successive peaks of MPF) as a function of the parameter *kampf* for MPF activation by CDC25P in the model of Qu et al.

the previous section, we concentrate here on the reverse effect of the cell cycle on the circadian clock by transcription inhibition during mitosis, for which the simpler two phase model of Qu et al. [18] is sufficient.

### 3.2 Models of the Circadian Clock

In many organisms, spontaneous gene expression oscillations with a period close to 24 hours have been observed. A biochemical clock present in each cell is responsible for maintaining these oscillations at this period. The central circadian clock in the suprachiasmatic nucleus (SCN) is sensitive to light and entrained by the day-night alternation, allowing molecular clocks in peripheral tissues to be synchronised by central signals. Indeed, Schibler and Nagoshi [8] have shown that in absence of synchronisation by the central clock, autonomous circadian oscillators are maintained in peripheral tissues with the same period, although they are progressively desynchronized.

In mammalian cells, two major proteins are transcribed in a circadian manner, CLOCK and BMAL1 which bind to form a heterodimer responsible for the transcription of several genes involved in intertwined feedback loops such as *Per* (Period), *Cry* (Cryptochrome), *Rev-Erb- $\alpha$*  or *Ror*. The newly-formed proteins then affect their own synthesis as PER and CRY associates to inhibit the activity of the complex CLOCK/BMAL1. REV-ERB- $\alpha$  has a similar effect and these two negative feedback loops give rise to sustained oscillations. Moreover, two positive feedback loops provided by the activation of *Bmal1* by ROR and the activation of *Cry* by REV-ERB- $\alpha$  are believed to bring more robustness to the oscillator.

In this paper we use the circadian clock model of Relogio et al. [19] which has been fitted on suprachiasmatic cells with precise data on the amplitude and phases of the different components. This model is composed of 20 species, 71 parameters, and all the feedback loops described above.

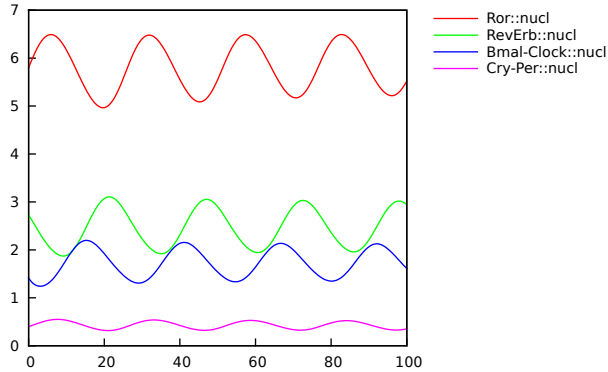


**Fig. 3.** Simulation of the Circadian Clock model of Relogio et al.

### 3.3 Coupling from the Cell Cycle to the Circadian Clock by the Inhibition of Transcription during Mitosis

It is known that in eukaryotes, gene transcription is significantly inhibited during mitosis [24]. In particular, the transcription inhibition of clock genes during mitosis and its impact on the circadian oscillator by shifting the phase of the circadian cycle has been shown in [15].

In this paper, we model the inhibition of clock genes transcription during mitosis with a negative Hill kinetics for mRNA synthesis taking the ratio between the concentrations of MPF and preMPF as inhibiting factor. The kinetics of mRNA synthesis reactions are thus modified as follows

$$S * \frac{J^n}{J^n + ([MPF]/[preMPF])^n}$$

where  $S$  is the original synthesis rate parameter in the model of Relogio et al. [19] and  $n$  is taken equal to 4 to mimic the abrupt inhibition of transcription when mitosis occurs. Transcription is thus inhibited when the ratio  $[MPF]/[preMPF]$  is high.

This modelling enforces the fact that for quiescent cells, whatever the FBS concentration, the transcription rate will be close to  $S$  and therefore the clock close to a period of 24h.

## 4 Computational Results

As shown in the right panel of Fig. 2, it is possible to simulate the experimental milieu enrichment with 10 or 15% FBS by varying the parameter  $kampf$  of the cell cycle model to obtain the same values for the period of the cell division cycle. The coupling of this model to the circadian clock uses two parameters:

the coupling strength  $J$ , and the order  $n$  of the Hill function. In the results reported in this section, we chose  $J = 2$  and  $n = 4$ , two of the smallest values found through our parameter search procedure.

Figure 4 shows the variation of the period of  $REV-ERB-\alpha$  when the two parameters  $kampf$  and  $J$  vary. The value of the period is captured with a temporal logic specification as seen in the subsection 2.2. Two domains can be distinguished in this parameter space: in the domain on the top left (above the black line) the clock keeps its period constant and close to 24h, thus it is not entrained. On the contrary, in the domain on the bottom right (below the black line) the clock is entrained to the same period as the cell cycle. One can see that using a different value for  $J$  would have led to different values for  $kampf$  in Table 2.

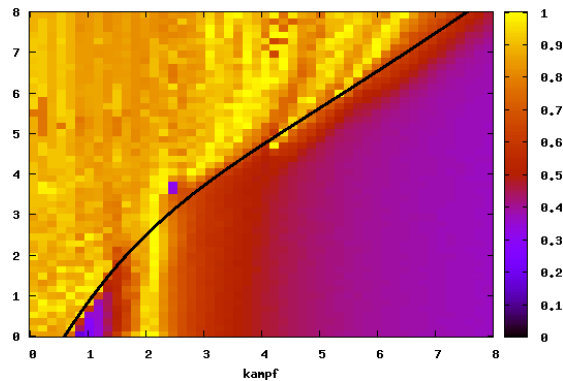


**Fig. 4.** Periods of  $REV-ERB-\alpha$  as a function of  $kampf$  for varying the cell cycle period,  $J$ , the strength of transcription inhibition during mitosis. Landscape computed as the satisfaction degree of the formula `distanceSuccPeaks([RevErb::nucl],[period],[transT])` which defines the period of  $REV-ERB-\alpha$  after a transient time  $transT=80$ , and with an objective of 24h for the *period*. Full satisfaction in yellow indicates a period of 24h for  $REV-ERB-\alpha$ , while the other colours indicate the absolute difference to 24h.

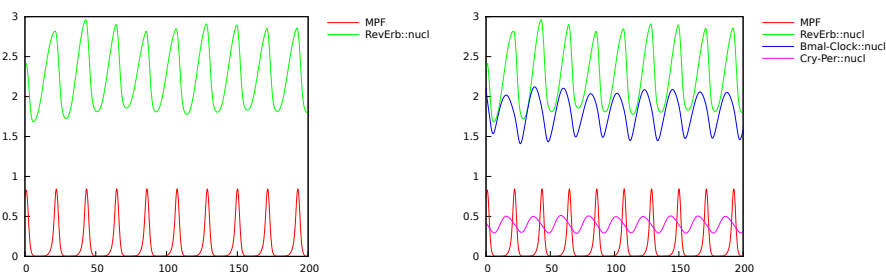
#### 4.1 Comparison to Experimental Data without Dexamethasone

Table 2 shows the periods of the circadian clock and the cell division cycle in our model with different values of  $kampf$  corresponding to the different culture conditions. In all cases, the cell division manages to entrain the circadian clock (that has a free period around 24h) to its period, simply through this mechanism of transcription inhibition, as depicted in Fig. 5 and Fig. 6 left panel. These simulation results reproduces quite well the data of table 1 when there

$kampf$	FBS %	Circadian clock period (h)	Cell division period (h)
3.75	10	21.43	21.30
12.1	15	18.60	18.60
1.6	5?	26.16	26.32

**Table 2.** Periods measured in the coupled model with different values of  $kampf$  for modeling the different culture conditions.

is no treatment by Dex. Note that our model can also have a cell division time higher than 24h, for instance with  $kampf=1.6$  which might correspond to a concentration of FBS around 5%. In that case we predict that the cell cycle will still entrain the circadian clock, lowering its period, even if our simulations show a longer transitory period, as depicted in Fig. 6 (right panel).



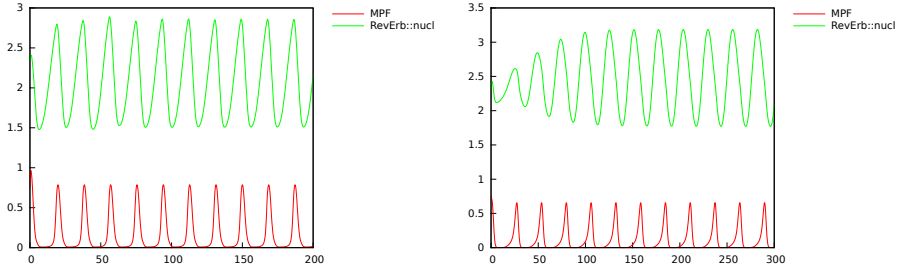
**Fig. 5.** Entrainment to a period around 21.3h with  $kampf = 3.75$  corresponding to a milieu enriched with 10% FBS. The same simulation including more clock genes is shown on the right to compare with Fig. 3.

## 4.2 Comparison to Data with Dexamethasone

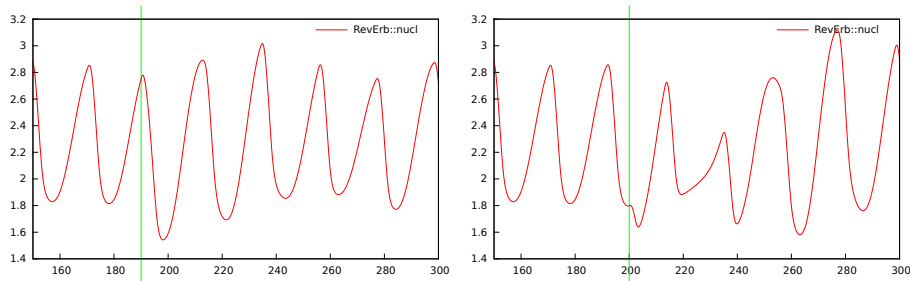
In order to take into account the experiments with Dexamethasone, the model can be extended with an event, lasting for two hours, and inducing *Per* mRNA while inhibiting the other clock genes.

Fig. 7 shows that in our models, regardless of the milieu (i.e. of the value of  $kampf$ ), the Dex pulse results in a perturbation of the clock and then returns to the observed entrainment.

These simulations point us to the possibility that the noisy data reported in Table 1 after the Dex pulse might simply be due to the various states in which the pulse happened and to the time necessary for the cells to recover their clock entrainment, rather than to two different oscillatory attractors of the system.



**Fig. 6. Left:** Entrainment to a period around 18.6h with  $kampf = 12.1$  corresponding to a milieu enriched with 15% FBS. **Right:** Entrainment to a period around 26.3h with  $kampf = 1.6$  corresponding to a poor milieu (FBS 5%?), as predicted by our model. Note that the Circadian clock takes more time to adjust to this lengthening of its period.



**Fig. 7.** Effect of a Dexamethasone pulse on the entrainment. The pulse alters the clock before returning to the previously observed entrainment regime. In the left panel the pulse is from time 190 to 192 while on the right it is from 200 to 202. The left panel's peak-to-peak distance remains in the  $[20.25, 22.3]$  interval, while the right one is in the  $[17.9, 24.1]$  interval. This might correspond to the two groups observed in [11]. The time to recover normal entrainment varies but is often larger than 72h.

A pulse at time 190h disrupted only slightly our clock, leading to mostly remaining in mode-locking 1:1, whereas postponing that same pulse by 10h (corresponding to giving the pulse to a cell in a different state) leads to a bigger disturbance, some peak-to-peak distances close to 24h, others to 17h, and even if this is transitory, this might correspond to the type of data observed in the Group 2 of Table 1.

### 4.3 Remaining Paradox on Phase Data

So far we have considered the periods of the circadian clock and the cell division cycle, but not their phase. The experimental data on the phase between the cell division time and the peak of REV-ERB- $\alpha$  protein in NIH3T3 fibroblast are quite consistent in Bieler et al. [3] and Feillet et al. [11] to indicate that the REV-ERB- $\alpha$  occurs 3-5 hours after cell division. However this is not the case in our coupled model where the peak of REV-ERB- $\alpha$  appears 17-20 hours after cell division, as shown in Table 3.

Medium	Experimental data	Model simulation
<b>FBS 5</b>	NA	18.6h
<b>FBS 10</b>	3.82h	20.7h
<b>FBS 15</b>	3.98	17.8h

**Table 3.** Phases as time delays, observed experimentally (without Dexamethasone) and by simulation, between the cell division time (peak of MPF in the simulations) and the appearance of a peak of concentration of REV-ERB- $\alpha$ .

Interestingly, a similar discrepancy appears in the model of Gerard and Goldbeter [12] which models the reverse effects of the circadian clock genes on the cell cycle, through Wee1, p21 and Cmyc, and shows mitosis gating. In their simulations, the peak of REV-ERB- $\alpha$  appears around 16 hours after cell division. We do not have explanations for these discrepancies between the computational models and the recent data which now permit to fit the models in phase in addition to periods.

In the circadian clock model of Relogio et al. [19], the phases of the different markers of the circadian clock have been precisely fitted to observations made in mice suprachiasmatic nucleus cells, however without data about cell divisions. On the other hand, in the data of Feillet et al.[11], REV-ERB- $\alpha$  is the only marker on the circadian clock and no comparison is thus possible with the other data.

## 5 Conclusion

Through a simple model for the transcription inhibition during mitosis, we have presented in this article the first mechanistic dynamical model demonstrating

the entrainment of the circadian clock by the cell division cycle. This model has been built on the ideas of [3] that the primary coupling between those two oscillators is from the cell division cycle to the circadian clock.

We have demonstrated that such a model is enough to reproduce the recently published biological data of [11] with different medium enrichment leading to different periods for mode-locked oscillators in dividing cells, whereas the quiescent cells still have a 24h clock. Our model also postulates a different interpretation of some of the results of that article when cells are treated by a 2h pulse of Dexamethasone: instead of different autonomous cycling regimes, the model predicts temporary perturbations leading to shorter or longer peak-to-peak distances, but returning to the previous entrainment regime after some time, longer than the horizon used in the experiments.

It is noteworthy that in our transcription-inhibition coupled models, the oscillations of the clock's core gene products are much sharper and their peaks closer in time (see for instance Figs. 3 and 5 right panel). Indeed, the peaks get "concentrated" outside of the time of transcription inhibition. A prediction of the model is therefore that in quickly dividing cells, the phase shifts between the different components of the clock are shorter than in quiescent cells where such a phenomenon should not occur.

Finally, though our rather simple model properly fits the data about the periods of the different cycles, the time difference observed between the peaks of MPF and of REV-ERB $\alpha$  is quite different in our model and in the experimental data. A similar discrepancy seems to also appear in the coupled model of [12]. More work is needed now to try to fit these models to the available phase data and probably create new data with several markers of the circadian clock in addition to cell division time.

**Acknowledgements.** This work has been funded by the ERASysBio+ project C5Sys through the ANR grant 2009-SYSB-002-02. We would like to thank all the partners of this project for fruitful discussions. This work was also granted access to the HPC resources of the CINES under the allocation c2015036437 made by GENCI.

## References

1. A. Ballesta, S. Dulong, C. Abbara, B. Cohen, A. Okyar, J. Clairambault, and F. Levi. A combined experimental and mathematical approach for molecular-based optimization of irinotecan circadian delivery. *PLOS Computational Biology*, 7(9), 2011.
2. J. W. Barnes, S. A. Tischkau, J. A. Barnes, J. W. Mitchell, P. W. Burgoon, J. R. Hickok, and M. U. Gillette. Requirement of mammalian timeless for circadian rhythmicity. *Science*, 302(5644):439–442, Oct. 2003.
3. J. Bieler, R. Cannavo, K. Gustafson, C. Gobet, D. Gatfield, and F. Naef. Robust synchronization of coupled circadian and cell cycle oscillators in single mammalian cells. *Molecular systems biology*, 10(7):739, Jan. 2014.

4. L. Calzone, N. Chabrier-Rivier, F. Fages, and S. Soliman. Machine learning biochemical networks from temporal logic properties. In G. Plotkin, editor, *Transactions on Computational Systems Biology VI*, volume 4220 of *Lecture Notes in Bioinformatics*, pages 68–94. Springer-Verlag, Nov. 2006. CMSB’05 Special Issue.
5. L. Calzone, F. Fages, and S. Soliman. BIOCHAM: An environment for modeling biological systems and formalizing experimental knowledge. *Bioinformatics*, 22(14):1805–1807, 2006.
6. L. Calzone and S. Soliman. Coupling the cell cycle and the circadian cycle. Research Report 5835, INRIA, Feb. 2006.
7. E. De Maria, F. Fages, A. Rizk, and S. Soliman. Design, optimization, and predictions of a coupled model of the cell cycle, circadian clock, dna repair system, irinotecan metabolism and exposure control under temporal logic constraints. *Theoretical Computer Science*, 412(21):2108–2127, May 2011.
8. N. Emi, S. Camille, B. Christoph, L. Thierry, N. Felix, and U. Schibler. Circadian gene expression in individual fibroblasts: cell-autonomous and self-sustained oscillators pass time to daughter cells. *Cell*, 119:693–705, 2004.
9. F. Fages and A. Rizk. On temporal logic constraint solving for the analysis of numerical data time series. *Theoretical Computer Science*, 408(1):55–65, Nov. 2008.
10. F. Fages and P. Traynard. Temporal logic modeling of dynamical behaviors: First-order patterns and solvers. In L. F. del Cerro and K. Inoue, editors, *Logical Modeling of Biological Systems*, chapter 8, pages 291–323. John Wiley & Sons, Inc., 2014.
11. C. Feillet, P. Krusche, F. Tamanini, R. C. Janssens, M. J. Downey, P. Martin, M. Teboul, S. Saito, F. a. Lévi, T. Bretschneider, G. T. J. van der Horst, F. Delaunay, and D. A. Rand. Phase locking and multiple oscillating attractors for the coupled mammalian clock and cell cycle. *Proceedings of the National Academy of Sciences of the United States of America*, 111(27):9928–9833, 2014.
12. C. Gérard and A. Goldbeter. Entrainment of the mammalian cell cycle by the circadian clock: Modeling two coupled cellular rhythms. *PLoS Comput Biol*, 8(21):e1002516, 05 2012.
13. L. Glass. Synchronization and rhythmic processes in physiology. *Nature*, 410(6825):277–84, Mar. 2001.
14. A. Gréchez-Cassiau, B. Rayet, F. Guillaumond, M. Teboul, , and F. Delaunay. The circadian clock component *bmal1* is a critical regulator of p21WAF1/CIP1 expression and hepatocyte proliferation. *J Biol Chem*, 283:4535–4542, 2008.
15. B. Kang, Y.-Y. Li, X. Chang, L. Liu, and Y.-X. Li. Modeling the effects of cell cycle m-phase transcriptional inhibition on circadian oscillation. *PLoS Comput Biol*, 4(3):e1000019, 03 2008.
16. T. Matsuo, S. Yamaguchi, S. Mitsui, A. Emi, F. Shimoda, and H. Okamura. Control mechanism of the circadian clock for timing of cell division in vivo. *Science*, 302(5643):255–259, Oct. 2003.
17. I. Perez-Roger. Myc activation of cyclin *e*/cdk2 kinase involves induction of cyclin *e* gene transcription and inhibition of p27(kip1) binding to newly formed complexes. *Oncogene*, 14(20):2373–81, 1997.
18. Z. Qu, W. R. MacLellan, and J. N. Weiss. Dynamics of the cell cycle: checkpoints, sizers, and timers. *Biophysics Journal*, 85(6):3600–3611, 2003.
19. A. Relógio, P. O. Westermark, T. Wallach, K. Schellenberg, A. Kramer, and H. Herzl. Tuning the mammalian circadian clock: robust synergy of two loops. *PLoS computational biology*, 7(12):e1002309, Dec. 2011.

20. A. Rizk, G. Batt, F. Fages, and S. Soliman. A general computational method for robustness analysis with applications to synthetic gene networks. *Bioinformatics*, 12(25):il69–il78, June 2009.
21. A. Rizk, G. Batt, F. Fages, and S. Soliman. Continuous valuations of temporal logic specifications with applications to parameter optimization and robustness measures. *Theoretical Computer Science*, 412(26):2827–2839, 2011.
22. P. Traynard, F. Fages, and S. Soliman. Trace simplifications preserving temporal logic formulae with case study in a coupled model of the cell cycle and the circadian clock (best student paper award). In *CMSB'14: Proceedings of the twelfth international conference on Computational Methods in Systems Biology*, number 8859 in Lecture Notes in Bioinformatics, pages 114–128. Springer-Verlag, Sept. 2014.
23. K. Ünsal-Kaçmaz, T. E. Mullen, W. K. Kaufmann, and A. Sancar. Coupling of human circadian and cell cycles by the timeless protein. *Molecular and Cellular Biology*, 25(8):3109–3116, Apr. 2005.
24. D. Weisenberger and U. Scheer. A possible mechanism for the inhibition of ribosomal rna gene transcription during mitosis. *Journal of Cell Biology*, May 1995.